Chemical Engineering Journal 154 (2009) 203–210

Contents lists available at ScienceDirect

Chemical Engineering Journal

journal homepage: www.elsevier.com/locate/cej

Initiator efficiency modeling for vinyl chloride suspension polymerization

Joris Wieme, Marie-Françoise Reyniers*, Guy B. Marin

Laboratorium voor Chemische Technologie, Ghent University, Krijgslaan 281 (S5), B-9000 Gent, Belgium

ARTICLE INFO

Article history:
Received 5 December 2008
Received in revised form 26 May 2009
Accepted 1 June 2009

Keywords:
Initiator efficiency
Suspension polymerization
Poly(vinyl chloride)

ABSTRACT

A unified methodology is developed to calculate the fraction of initiator derived radicals that initiates the polymerization, i.e. the initiator efficiency, as a function of polymerization time and polymerization conditions. In the presented approach the most important reactions that initiator derived radicals undergo are taken into account. All involved parameters have a clear physical and fundamental meaning and no adjustment to experimental data is required. The presented methodology is applied to diacyl peroxide initiators that are commonly used in industrial vinyl chloride suspension polymerization processes: dodecanoyl peroxide and benzoyl peroxide. Validation is performed by comparing calculated and experimental data for the monomer conversion and averages of the molar mass distribution within a polymerization temperature range of 323–333 K and an initiator concentration range of 0.26–4.2 wt% based on the monomer.

1. Introduction

It is well known that suspension polymerization processes virtually stop before a complete conversion of 100% is reached [1]. This can be explained in terms of the so-called cage effect [1,2]. The latter pertains to a lowering at high monomer conversions of the initiator efficiency, i.e. the fraction of initiator derived radicals that initiates the polymerization [3]. After dissociation, the radicals obtained from an initiator molecule are still in close proximity to one another and their recombination is possible. The probability of this recombination increases when diffusion is hampered, i.e. at high monomer conversions [4]. If the initiator dissociation is accompanied by the escape of a small molecule from the solvent cage, as e.g. in decarboxylation by a concerted two-bond scission or by β-scission, recombination of the radicals results in the formation of an inert molecule and, hence, in a lower than 100% efficiency of the initiator.

The efficiency of an initiator depends on its decomposition mechanism, on the composition of the polymerization mixture and on the polymerization temperature. It is generally accepted that assigning a constant value to the initiator efficiency during the polymerization process can lead to significant errors in both monomer conversion and molar mass distribution (MMD) calculations [5], especially at higher monomer conversions (≥ 80%) [6,7].

In vinyl chloride suspension polymerization modeling, the majority of the initiator efficiency models consider the initiator efficiency in the monomer-rich phase, f_1, equal to an intrinsic initiator efficiency (i.e. $f_1 = f_{chem}$), whereas the initiator efficiency in the polymer-rich phase, f_2, is built up from an intrinsic contribution (f_{chem}) and a diffusional contribution ($k_{f,diff}$) [8,4]:

$$\frac{1}{f_2} = \frac{1}{f_{chem}} + \frac{1}{k_{f,diff}} \quad (1)$$

Some of the parameters required in Eq. (1) are considered to be adjustable and, hence, need to be fitted to experimental data in order to allow for a correct description of the initiator efficiency. An established method to calculate the diffusion contribution to the apparent initiator efficiency, $k_{f,diff}$ in Eq. (1), is presented by De Roo et al. [4], leading to the following expression for the apparent initiator efficiency f_2:

$$\frac{1}{f_2} = \frac{1}{f_{chem}} + \frac{1}{8\pi\sigma_m N_A D_{i,2}} \quad (2)$$

in which σ_m is taken equal to the Lennard–Jones diameter of a monomer molecule, N_A is the Avogadro constant and $D_{i,2}$ the diffusion coefficient of an initiating radical in the polymer-rich phase.

On the other hand, Kurdikar and Peppas [9] developed a method without adjustable parameters to calculate the initiator efficiency for UV polymerization processes using the 2,2-dimethoxy-2-phenylacetophenone initiator. The model introduced by these authors allows for an a priori calculation of the initiator efficiency by taking into account the most important decomposition reactions of the initiator. The resulting model equations are a function of intrinsic kinetic parameters related to the initiator decomposition and of the initiating radical diffusion coefficients. Hence, provided these intrinsic kinetic parameters are known and these diffusion coefficients can be calculated, the developed model allows to calculate the initiator efficiency as a function of polymerization time and

* Corresponding author. Tel.: +32 9 264 4516; fax: +32 9 264 4999.
E-mail address: mariefrancoise.reyniers@ugent.be (M.-F. Reyniers).

1385-8947/$ – see front matter © 2009 Elsevier B.V. All rights reserved.
doi:10.1016/j.cej.2009.06.004

Nomenclature

A	pre-exponential factor of intrinsic rate coefficient [$m^3\ mol^{-1}\ s^{-1}$] or [s^{-1}]
$D_{i,2}$	initiator derived radical self-diffusion coefficient in the polymer-rich phase [$m^2\ s^{-1}$]
D_x^*	mutual diffusion coefficient of radical pair x ($x = A,\ B$) [$m^2\ s^{-1}$]
E^*	activation energy to make a diffusional jump [$J\ mol^{-1}$]
E_a	activation energy of intrinsic rate coefficient [$J\ mol^{-1}$]
f_{chem}	intrinsic initiator efficiency
f_k	initiator efficiency in phase k
F_x	conditional probability that primary radicals escape recombination inside ($x = in$) or outside the solvent cage ($x = out$)
$k_{f,diff}$	diffusion contribution to the initiator efficiency in the polymer-rich phase
$k_{x,chem}$	Intrinsic rate coefficient reaction x ($x = bd, p, r, \beta$ [s^{-1} or $m^3\ mol^{-1}\ s^{-1}$]
M	monomer concentration [$mol\ m^{-3}$]
M_m	mass averaged molar mass of polymer molecules [$kg\ mol^{-1}$]
M_n	number averaged molar mass of polymer molecules [$kg\ mol^{-1}$]
M_z	z averaged molar mass of polymer molecules [$kg\ mol^{-1}$]
N_A	Avogadro number [mol^{-1}]
p_x	recombination probability of a radical pair x ($x = A,\ B$) over the investigated time range
r	relative distance between two radicals [m]
r_0	initial relative distance between two radicals [m]
R	universal gas constant / total macroradical concentration [$J\ mol^{-1}\ K^{-1}$/$mol\ m^{-3}$]
t	polymerization time [s]
T	temperature [K]

Greek symbols

γ	average overlap factor for the hole free volume of the mixture
σ_m	Lennard–Jones diameter of a monomer molecule [m]
σ_x	reaction distance for recombination of radical pair x ($x = A,\ B$) [m]
$\phi_x(r, t)$	probability per unit of finding radicals of pair x ($x = A,\ B$) at a distance r from each other at a time t [m^{-3}]

Subscripts

bd	bond dissociation
p	propagation
r	recombination
β	β-scission

polymerization conditions. However, up until now this method has not been used to simulate the polymerization process by coupling it to a kinetic model describing the polymerization kinetics.

In this work the initiator efficiency model of Kurdikar and Peppas [9] is coupled with a kinetic model describing the vinyl chloride suspension polymerization kinetics for two diacyl peroxide initiators commonly used in industrial practice, i.e. dodecanoyl peroxide (also called lauroyl peroxide, LPO) and benzoyl peroxide (BPO). The intrinsic rate coefficients for the initiation and the polymerization reaction steps are taken from literature, while the diffusion coefficients are calculated using the free volume theory. To the best of our knowledge, this is the first time that this modeling approach is applied to account for the variation of the initiator efficiency in both phases of the vinyl chloride suspension polymerization process.

Validation of this methodology is performed by comparing calculated monomer conversions and averages of the molar mass distribution (MMD) as a function of polymerization time and process conditions with experimental data reported in literature. Also, a comparison of the initiator efficiency model of Kurdikar and Peppas [9] and the semi-empirical model of De Roo et al. [4](Eq. (2)) is presented.

2. Model equations

2.1. Mass balances and moment equations

The vinyl chloride suspension polymerization is modeled using a two-phase model, as described in detail by De Roo et al. [4]. The reactions taken into account in the modeling of the vinyl chloride suspension polymerization are shown in the supporting information (Table S.1). The considered reaction scheme holds in both the monomer-rich and the polymer-rich phase. The bimolecular reactions in the polymer-rich phase are considered to become possibly diffusion controlled, whereas the reactions in the monomer-rich phase are considered to be reaction controlled. The rate coefficients of the bimolecular reactions in the polymer-rich phase are calculated as apparent rate coefficients built up from an intrinsic and a diffusion contribution [2,4]. The Arrhenius parameters of the intrinsic rate coefficients k_{chem} of all polymerization reactions shown in Table S.1 were taken from De Roo et al. [4] and are given in the supporting information (Table S.2).

The mass balances for the monomer, the initiator radicals, the macroradicals and the polymer molecules are also given in the supporting information. The concentration of the initiator derived radicals and the chlorine radicals is obtained by applying the quasi-steady state approximation to these species. The method of moments is applied to calculate the average properties of the MMD (M_n, M_m, M_z). This reduces the number of balances to be solved. The equations for the moments of the macroradical and the polymer distribution are given in Table S.4. The mass balances for the initiator and the monomer are also given in this table as the moment equations are integrated together with these mass balances.

2.2. Initiator efficiency calculation

In this section an analytical expression to calculate the initiator efficiency in both phases of the vinyl chloride suspension polymerization process is derived based on the methodology presented by Kurdikar and Peppas [9]. In order to enable a correct description of the initiator efficiency, the initiator decomposition kinetics need to be accounted for. Fig. 1 shows a schematic of the decomposition mechanism of a typical initiator that undergoes a two-bond dissociation reaction. According to this mechanism two bonds are broken simultaneously, resulting in the formation of two initiator radicals A and A_1 and a small molecule C, typically CO_2. If the radical pair A and A_1 fails to diffuse out of the solvent cage, recombination into a molecule I_1 is possible. The solvent cage is defined as the region around the radical A within which recombination with radical A_1 may occur if this radical is found in that region. The radical A_1 may decompose to form another radical B and a molecule C'. The radical pair A and B can also recombine to form a molecule I_2. If the recombination reactions of A with A_1 and A with B result in the formation of inert molecules I_1 and I_2, as is the case for the investigated diacyl peroxides, these reactions are the primary cause of the decrease of the initiator efficiency. For the radicals to be able to initiate chains, the radicals must, once they have escaped the solvent cage, initi-

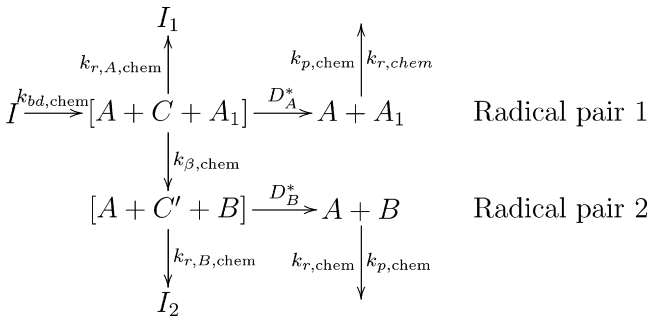

Fig. 1. Decomposition scheme of diacyl peroxide initiators [9]. *I* is the initiator molecule; *A*, A_1, *B* are initiator derived radicals; I_1 and I_2 are inert recombination products, *C* and *C*′ are non-radical species resulting from two-bond dissociation and β-scission reaction.

ate chains as opposed to terminate growing chains. Thus, following Kurdikar and Peppas [9], the initiator efficiency, *f*, can be written as

$$f = F_{\mathrm{in}} F_{\mathrm{out}} \tag{3}$$

F_{in} is the probability that primary radicals do not recombine within the solvent cage. F_{out} is the conditional probability that the initiator derived radicals initiate chains rather than terminate growing chains once they escape the solvent cage, the so-called propagation probability.

F_{out} can be obtained from

$$F_{\mathrm{out}} = \frac{k_{p,\mathrm{chem}} M}{k_{p,\mathrm{chem}} M + k_{r,\mathrm{chem}} R} \tag{4}$$

where *M* is the monomer concentration, *R* is the total macroradical concentration and $k_{p,\mathrm{chem}}$ and $k_{r,\mathrm{chem}}$ are the intrinsic rate coefficients for propagation and for termination by recombination. F_{out} is close to 1 throughout the polymerization process as the monomer concentration is several orders of magnitude higher than the radical concentration and this even at very high monomer conversions.

F_{in} can be obtained from

$$F_{\mathrm{in}} = F_{\mathrm{in},A} F_{\mathrm{in},B} \tag{5}$$

where $F_{\mathrm{in},A}$ is the probability that *A* and A_1 will avoid recombination and $F_{\mathrm{in},B}$ is the probability that *A* and *B* will avoid recombination [9].

Let $\phi_A(r, t)$ be the probability per unit volume of finding an A_1 radical at distance *r* from an *A* radical at time *t*. Fixing the frame of reference on the *A* radical, while assuming an axissymmetric situation, allows to write a balance for A_1 outside the solvent cage of radius σ_A

$$\frac{\partial \phi_A}{\partial t} = D_A^* \left(\frac{\partial^2 \phi_A}{\partial r^2} + \frac{2}{r} \frac{\partial \phi_A}{\partial r} \right) - k_{\beta,\mathrm{chem}} \phi_A - 2K\phi_A \tag{6}$$

where D_A^* is the mutual diffusion coefficient given by the sum of the diffusion coefficients of radicals *A* and A_1 ($D_A^* = D_A + D_{A_1}$). $k_{\beta,\mathrm{chem}}$ in Eq. (6) is the rate coefficient of the β-scission reaction converting radical A_1 into radical *B* and *K* is given by

$$K = k_{p,\mathrm{chem}} M + k_{r,\mathrm{chem}} R \tag{7}$$

The first term on the right hand side of Eq. (6) accounts for the diffusion of radical pair *A* and A_1, while the second and third term represent the disappearance of radical pair *A* and A_1 by reaction. The second term accounts for the β-scission reaction which converts radical A_1 into radical *B*, while the third term accounts for the reaction of *A* and A_1 with monomer and macroradicals present in the reaction mixture.

Let the initial distance of separation between *A* and A_1 radicals be r_0. The corresponding initial conditions can then be written as

$$\phi_A(r, 0) = 0 \quad \forall r \neq r_0 \tag{8}$$

$$\phi_A(r_0, 0) = 1 \tag{9}$$

The boundary conditions can be written as

$$4\pi\sigma_A^2 N_A D_A^* \left(\frac{\partial \phi_A}{\partial r} \right)_{r=\sigma_A} = k_{r,A,\mathrm{chem}} \phi_A(\sigma_A, t) \tag{10}$$

$$\phi_A(\infty, t) = 0 \tag{11}$$

with $k_{r,A,\mathrm{chem}}$ the intrinsic rate coefficient for the recombination reaction of *A* and A_1. The first boundary condition (Eq. (10)) expresses that not all collisions lead to reaction [10]. The second boundary condition reflects that, because the probability of propagation outside the solvent cage is very high, the probability that radicals *A* and A_1 are able to diffuse apart until they are infinitely far from each other is zero.

A similar expression is obtained for $\phi_B(r, t)$, the probability per unit volume of locating a *B* radical at a distance *r* from an *A* radical at time *t*. Writing a balance for *B* outside the solvent cage of radius σ_B results in

$$\frac{\partial \phi_B}{\partial t} = D_B^* \left(\frac{\partial^2 \phi_B}{\partial t^2} + \frac{2}{r} \frac{\partial \phi_B}{\partial r} \right) + k_{\beta,\mathrm{chem}} \phi_A - 2K\phi_B \tag{12}$$

Here, D_B^* is the mutual diffusion coefficient of *A* and *B*, given by the sum of the diffusion coefficients of *A* and *B* ($D_B^* = D_A + D_B$). Initially, no *B* radicals are present, therefore the corresponding initial condition is given by

$$\phi_B(r, 0) = 0 \quad \forall r \tag{13}$$

The boundary conditions are given by

$$4\pi\sigma_B^2 N_A D_B^* \left(\frac{\partial \phi_B}{\partial r} \right)_{r=\sigma_B} = k_{r,B,\mathrm{chem}} \phi_B(\sigma_B, t) \tag{14}$$

$$\phi_B(\infty, t) = 0 \tag{15}$$

with $k_{r,B,\mathrm{chem}}$ the intrinsic rate coefficient for the recombination reaction of *A* and *B*.

The probability of recombination of 1 pair *A* and A_1 (p_A) and *A* and *B* (p_B) radicals over the entire investigated time range is given by

$$p_A = \frac{k_{r,A,\mathrm{chem}}}{N_A} \int_0^\infty \phi_A(\sigma_A, t)\mathrm{d}t \tag{16}$$

$$p_B = \frac{k_{r,B,\mathrm{chem}}}{N_A} \int_0^\infty \phi_B(\sigma_B, t)\mathrm{d}t \tag{17}$$

The initiator efficiency is then given by

$$f = F_{\mathrm{out}}(1 - p_A)(1 - p_B) \tag{18}$$

As the set of partial differential equations and corresponding initial and boundary conditions is linear and the coefficients can be assumed constants, an analytical solution can be obtained for p_A and p_B [9]:

$$p_A = \frac{k_{r,A}^* \sigma_A^2 e^{\sqrt{\frac{k_{\beta,\mathrm{chem}}+2K}{D_A^*}}(\sigma_A - r_0)}}{r_0 \left(D_A^* + k_{r,A}^* \sigma_A + \sigma_A \sqrt{(k_{\beta,\mathrm{chem}} + 2K) D_A^*} \right)} \tag{19}$$

$$p_B = \alpha \frac{D_1 - D_2}{N_1 N_2 N_3} \tag{20}$$

in which α, D_1, D_2, N_1, N_2 and N_3 are given by

$$\alpha = \frac{k_{r,B}^* k_{\beta,\mathrm{chem}} \sigma_B^2}{r_0} \tag{21}$$

$$D_1 = \left(D_B^* D_A^* + \sqrt{2D_B^* K} D_A^* \sigma_A + D_B^* k_{r,A}^* \sigma_A \right) e^{\sqrt{\frac{k_{\beta,\mathrm{chem}}+2K}{D_A^*}}(\sigma_A - r_0)} \tag{22}$$

Table 1
Values of the Arrhenius parameters of the intrinsic rate coefficients for the bond dissociation reaction $k_{\beta,\text{chem}}$ and for the β-scission reaction $k_{\beta,\text{chem}}$ for dodecanoyl peroxide (LPO) and benzoyl peroxide (BPO) [12–14].

	Bond dissociation		β-Scission	
	A [s^{-1}]	E_a [kJ mol^{-1}]	A [s^{-1}]	E_a [kJ mol^{-1}]
LPO	3.92×10^{14}	123.37	1.0×10^{14}	45.7
BPO	9.34×10^{15}	139.0	1.0×10^{14}	45.7

$$D_2 = \left(D_A^* + \sqrt{D_A^* \left(k_{\beta,\text{chem}} + 2K \right)} \sigma_A + k_{r,A}^* \sigma_A \right) e^{\sqrt{\frac{2K}{D_B^*}} (\sigma_A - r_0)} \quad (23)$$

$$N_1 = D_A^* + \sqrt{D_A^* \left(k_{\beta,\text{chem}} + 2K \right)} \sigma_A + k_{r,A}^* \sigma_A \quad (24)$$

$$N_2 = D_B^* + \sqrt{2 D_B^* K} \sigma_A + k_{r,B}^* \sigma_A \quad (25)$$

$$N_3 = 2K D_A^* - \left(k_{\beta,\text{chem}} + 2K \right) D_B^* \quad (26)$$

in which

$$k_{r,X}^* = \frac{k_{r,X,\text{chem}}}{4\pi \sigma_X^2 N_A} \quad X = A, B$$

2.3. Intrinsic rate coefficients and diffusion coefficients

In this study all intrinsic kinetic parameters pertaining to the polymerization reactions and to the initiator decomposition reactions have been taken from literature. Hence, no adjustment of any kinetic parameter to experimental data has been performed. The Arrhenius parameters of the intrinsic rate coefficients of the polymerization reactions have been taken from De Roo et al. [4] and are shown in Table S.2. The values for the Arrhenius parameters of the intrinsic rate coefficients of the bond dissociation reaction, $k_{bd,\text{chem}}$, are given in Table 1 for all considered initiators. The $k_{bd,\text{chem}}$ values reported by Moad and Solomon [11] are used. Values for the β-scission rate coefficient ($k_{\beta,\text{chem}}$) for the considered initiators were taken from literature [12–14] and are also given in Table 1.

The recombination rate coefficients $k_{r,\text{chem}}$, $k_{r,A,\text{chem}}$ and $k_{r,B,\text{chem}}$ and the addition rate coefficient $k_{p,\text{chem}}$ were taken equal for all considered initiators. $k_{r,\text{chem}}$, the rate coefficient for the recombination of a macroradical and an initiator derived radical was taken equal to the intrinsic termination by recombination rate coefficient as shown in Table S.2. The intrinsic rate coefficient of the addition of an initiator derived radical to monomer, $k_{p,\text{chem}}$, was taken equal to the intrinsic propagation rate coefficient as shown in Table S.2. $k_{r,A,\text{chem}}$ and $k_{r,B,\text{chem}}$ were taken equal to 1.0×10^5 m^3 mol^{-1} s^{-1}, as reported by Kochi [15]. Note that the intrinsic recombination rate coefficients were considered to be temperature independent, in agreement with De Roo et al. [4]. The diffusion coefficients of the radicals are calculated using the free volume theory. For more details on the diffusion coefficient calculation reference is made to De Roo et al. [4] and the supporting information (Section S.5).

3. Model validation

In the following section the initiator efficiency model as described in Section 2.2 is validated. First, model calculations are compared to experimental data concerning monomer conversion and averages of the molar mass distribution (Section 3.1) for vinyl chloride suspension polymerization processes for two commonly used diacyl peroxide initiators, i.e. dodecanoyl peroxide (LPO) and benzoyl peroxide (BPO). Next, the proposed initiator efficiency model is compared to model calculations using the initiator efficiency model presented in Eq. (2)[4](Section 3.2). The reaction conditions used in the calculations are given in Table 2. Note that the temperatures mentioned in Table 2 are polymerization temperatures. These temperatures are reached after a short heating period at the start of the polymerization process, which is explicitly accounted for in the model calculations.

Table 2
Reaction conditions of the vinyl chloride suspension polymerization experiments performed with different peroxide initiators.

Reaction condition	Units	Initiator		
		LPO [a]	LPO [b]	BPO [b]
Temperature	[K]	333	323	323
Initiator concentration (based on monomer)	[wt%]	0.26	0.53, 1.0, 2.2, 4.2	0.8, 2, 4

[a] Cebollada et al. [16].
[b] Crosato-Arnaldi et al. [17].

3.1. Experimental validation

3.1.1. Dodecanoyl peroxide

For dodecanoyl peroxide, LPO, experimental results have been reported in the concentration range of 0.53–4.21 wt%, based on the monomer [17]. Cebollada et al. [16] provide data for monomer conversion and averages (M_n, M_m) of the MMD at a temperature of 333 K using 0.26 wt% of initiator, based on the monomer (see Table 2).

The calculated and experimental monomer conversion as a function of polymerization time for both references and the averages of the MMD from Cebollada et al. [16] are shown in Figs. 2 and 3. A good agreement is obtained between calculated and experimental values.

In Figs. 2(a) and 3 the initiator efficiency in the monomer-rich, f_1, and in the polymer-rich phase, f_2, are presented as a function of polymerization time. During the heating of the reactor, both f_1 and f_2 first increase to reach a constant value. The increasing temperature leads to an increase of the diffusion coefficients, both in the monomer-rich and in the polymer-rich phase. As the recombination reactions are not activated, the corresponding rate coefficients remain constant. Therefore, during the heating of the reactor, the relative importance of the termination reactions decreases, causing an increase of the initiator efficiency.

From Figs. 2(a) and 3 t is clear that the value of f_1 is higher than the value of f_2 at all times. This is explained by the higher diffusion coefficients in the monomer-rich phase as compared to the polymer-rich phase. Initiator derived radicals can more easily diffuse apart in the monomer-rich phase, hence resulting in a higher value of the initiator efficiency f_1.

Since during the second stage of the polymerization (i.e. monomer conversions lower than ≈ 70%) the temperature and the composition of the polymer-rich phase remain constant [4], the diffusion coefficients of the initiator derived radicals and the rate coefficients will remain constant throughout the second stage of the polymerization and, hence, the value of the initiator efficiency in the polymer-rich phase does not change until the start of the third stage of the polymerization (i.e. monomer conversions higher than ≈ 70%). From the start of the third stage of the polymerization process on, the viscosity of the polymer-rich phase increases because the monomer concentration is now decreasing in this phase. This implies that diffusion becomes more and more difficult, hence increasing the probability of recombination of initiator derived radicals.

The described variation of the initiator efficiency in the polymer-rich phase as a function of monomer conversion induces variations of the rate of initiation and, hence, the total radical concentration in the polymer-rich phase. The decrease of the initiator efficiency during the third stage of the polymerization therefore determines the final conversion of the polymerization process. Fig. 4 shows

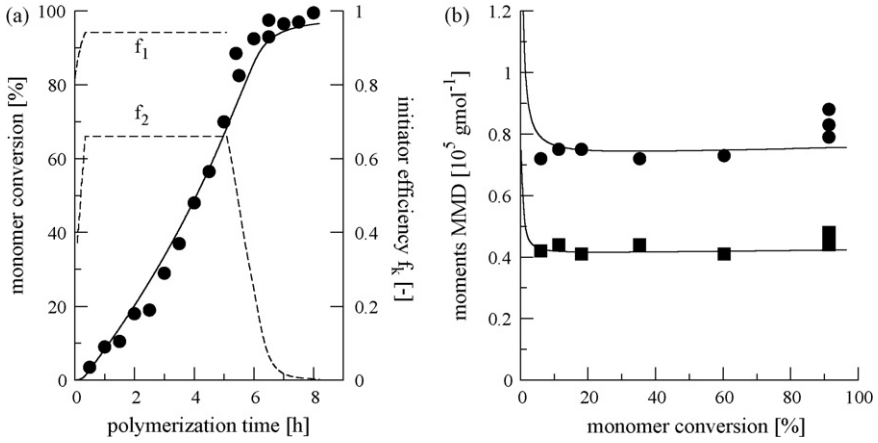

Fig. 2. (a) Monomer conversion and initiator efficiency f_k ($k = 1, 2$) as a function of polymerization time and (b) averages of the MMD as a function of monomer conversion in vinyl chloride suspension polymerization with initiator dodecanoyl peroxide (LPO). Experimental: (a) ●, monomer conversion; (b) ●, M_m; ■, M_n. Calculated: (a) (solid line) monomer conversion; (dashed line) initiator efficiency f_k; (b) averages of the MMD. Solid lines calculated by integration of equations in Table S.4 with the set of intrinsic Arrhenius parameter values given in Table S.2; f_k calculated from Eq. (18) with Arrhenius parameters as shown in Table 1. Polymerization temperature 333 K, initiator concentration 0.26 wt% based on the monomer. [16].

the total radical concentration and the net radical formation rate in the polymer-rich phase throughout the polymerization process for the polymerization conditions as reported by Cebollada et al. [16]. The net radical formation rate is calculated as the difference between the initiation and termination rate. An initial increase of the net radical formation rate in the polymer-rich phase is observed in Fig. 4. This initial increase can be explained by the increase of the temperature at the beginning of the polymerization process. Due to the temperature dependence of both the intrinsic initiator decomposition rate coefficient and the initiator efficiency, the radical formation rate increases, whereas the intrinsic termination rate coefficient is temperature independent. This increasing net radical formation rate corresponds to an increase of the radical concentration. As the radical concentration increases, the termination rate increases and the net radical formation rate reaches a maximum and then decreases to a constant value during the second stage of the polymerization process (i.e. up to monomer conversions of ≈ 70%).

As can be seen from Fig. 4, from the start of the third stage onwards, after approximately 5 h, more radicals are formed as the macroradical termination rate decreases more rapidly than the initiation rate. As polymerization goes on, however, the initiator efficiency, and hence the initiation rate, decreases more rapidly, resulting in a maximum value of the radical concentration. At even higher polymerization times, less radicals are initiated than terminated (i.e. f_2 reaches a value of 0), resulting in a decreasing radical concentration. Due to this decreasing radical concentration the polymerization rate decreases and the polymerization process ceases.

From Fig. 3 it is also clear that higher initiator concentrations result in a faster increase of the monomer conversion profile. The higher initiator concentrations result in a faster production of radicals and, hence, higher radical concentrations. These higher radical concentrations subsequently increase the polymerization rate.

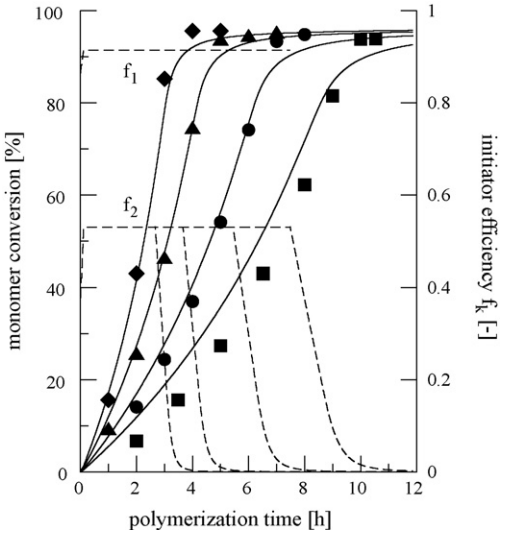

Fig. 3. Monomer conversion and initiator efficiency f_k ($k = 1, 2$) as a function of polymerization time in vinyl chloride suspension polymerization with initiator dodecanoyl peroxide (LPO). Experimental: ■, 0.53 wt%; ●, 1.0 wt%; ▲, 2.16 wt%; ♦, 4.21 wt% initiator. Calculated: (solid lines) monomer conversion, calculated by integration of equations in Table S.4 with the set of intrinsic rate coefficients as shown in Table S.2; (dashed lines) initiator efficiency f_k, calculated using Eq. (18) with Arrhenius parameters as shown in Table 1. Polymerization temperature 323 K, reaction conditions are given in Table 2[17].

3.1.2. *Benzoyl peroxide*

Suspension polymerization experiments at 323 K with the initiator benzoyl peroxide in the concentration range 0.8–4 wt% are

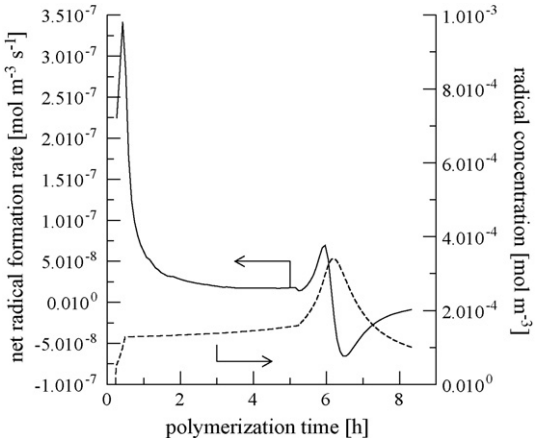

Fig. 4. Full line: net radical formation rate in polymer-rich phase; dashed line: radical concentration in polymer-rich phase. All lines calculated by integration of equations in Table S.4. Reaction conditions as mentioned in Table 2.

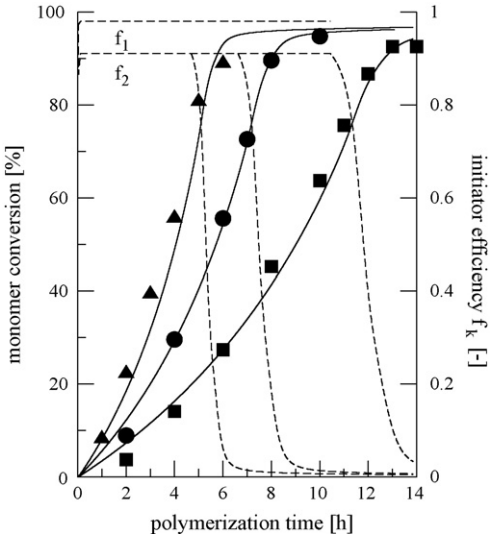

Fig. 5. Monomer conversion and initiator efficiency f_k ($k = 1, 2$) as a function of polymerization time in vinyl chloride suspension polymerization with initiator benzoyl peroxide (BPO). Experimental: ■, 0.8 wt%; ●, 2.0 wt%; ▲, 4.0 wt% initiator. Calculated: (solid lines) monomer conversion, calculated by integration of equations in Table S.4 with the set of intrinsic Arrhenius parameter values given in Table S.2; (dashed lines) initiator efficiency f_k, calculated from Eq. (18) with Arrhenius parameters as shown in Table 1. Polymerization temperature 323 K, reaction conditions are given in Table 2.

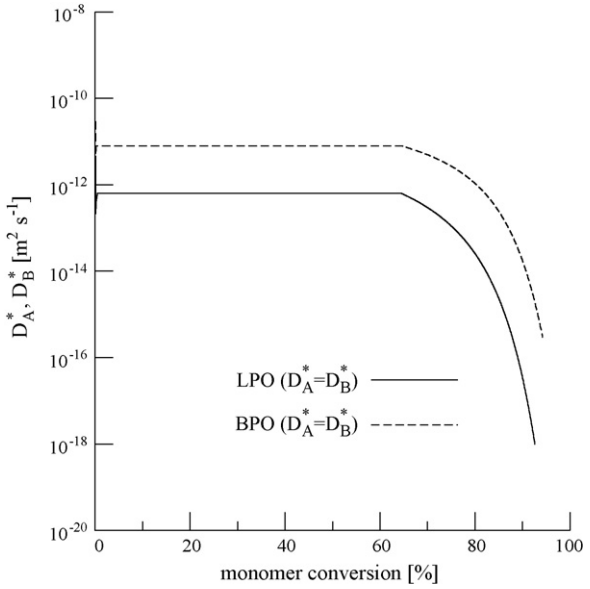

Fig. 6. Mutual diffusion coefficients of the radical pairs formed during the decomposition of dodecanoyl peroxide (LPO) and benzoyl peroxide (BPO) in the polymer-rich phase. Diffusion coefficients calculated from Eq. (S.18) in the Supporting Information section; polymerization temperature 323 K.

available from Crosato-Arnaldi et al. [17]. The calculated and experimental monomer conversion as a function of polymerization time are shown in Fig. 5. As can be seen, a good agreement is obtained. The initiator efficiency in both phases, f_1 and f_2, first increases as a function of polymerization time during the heating period and then remains constant. As for the dodecanoyl peroxide initiator, the initiator efficiency in the polymer-rich phase, f_2, remains constant until the start of the third stage. Compared to the initiator efficiency of dodecanoyl peroxide, both the f_1 value and the f_2 value in the plateau region for benzoyl peroxide are higher. At 323 K, the f_1 value for dodecanoyl peroxide is 0.91, whereas the value for benzoyl peroxide is 0.98. The f_2 value for dodecanoyl peroxide is 0.53, whereas the value for benzoyl peroxide is 0.91. This higher value for the initiator efficiency of benzoyl peroxide can be explained by the smaller initiator derived radicals in the case of benzoyl peroxide. This implies that the mutual diffusion coefficients D_A^* and D_B^* are higher in the case of benzoyl peroxide, as can be seen from Fig. 6. The higher mobility of the initiator derived radicals is the main cause for the higher value of the initiator efficiency. The higher values of D_A^* and D_B^* for benzoyl peroxide, compared to the values for lauroyl peroxide also explain the higher difference between f_1 and f_2 for the latter.

3.2. Comparison of initiator efficiency models

In this section the initiator efficiency model described in Section 2.2 is compared to the methodology presented by De Roo et al. [4](Eq. (2)). This is done for both initiators discussed in Section 3.1 by calculating the monomer conversion and averages of the MMD using both initiator models. Both calculation results are subsequently compared with each other and with experimental data.

For the calculation of the initiator efficiency based on Eq. (18) reference is made to Section 2.2. For the calculation of the initiator efficiency based on Eq. (2) the specification of f_{chem} is required. For dodecanoyl peroxide (LPO) a f_{chem} value of 0.7 has been used in agreement with the reported range of 0.65–0.82 by Moad and Solomon [11]. For the benzoyl peroxide initiator (BPO) f_{chem} was taken equal to 1, according to Crosato-Arnaldi et al. [17]. It should be stressed that the assignment of f_{chem} is a major weakness of this initiator efficiency model as no strong argumentation is available for the selection of this value. f_{chem} in Eq. (2) can therefore be considered an adjustable parameter that should be fitted to experimental data.

3.2.1. Dodecanoyl peroxide initiator (LPO)

Fig. 7 shows for the LPO initiator a comparison of experimental data for the monomer conversion and the averages of the MMD with calculated profiles using both initiator efficiency models. The full lines in this figure represent calculations based on the initiator efficiency model presented in Eq. (18) in Section 2.2, whereas the dashed lines correspond to Eq. (2). As can be seen in both cases a good agreement with experimental data is obtained. From Fig. 7(a) and (b) it becomes clear that the calculated conversion profiles differ whereas the averages of the MMD are rather invariant towards a change of the initiator efficiency model.

The calculated initiator efficiency profiles are also shown in Fig. 7(a). From this figure it can be concluded that some major differences occur between both models. Firstly, based on Eq. (2)(dashed line), the initiator efficiency in the monomer-rich phase f_1 is constant and equal to the proposed intrinsic initiator efficiency f_{chem} of 0.7. Note that f_1 and f_2 from Eq. (2) coincide until the start of the third stage of the polymerization process. This is in sharp contrast with the f_1 value resulting from the model presented in Section 2.2(Eq. (18), solid line), which varies as a function of polymerization time at the initial stages of the polymerization process. This variation can be explained in terms of the increasing polymerization temperature at the start of the polymerization process, as discussed into detail in Section 3.1. From Fig. 7(a) it also becomes clear that different values for f_1 are obtained using both methodologies. A value of 0.94 is obtained for f_1 based on Eq. (18)(dashed line), which is considerably higher than the value 0.7 as obtained from Eq. (2)(solid line).

The initiator efficiency in the polymer-rich phase, f_2, also differs significantly. At low monomer conversions both calculated f_2 values are comparable: 0.7 based on Eq. (2)(dashed line) as compared to 0.66 based on Eq. (18)(solid line). However, the calculated value of

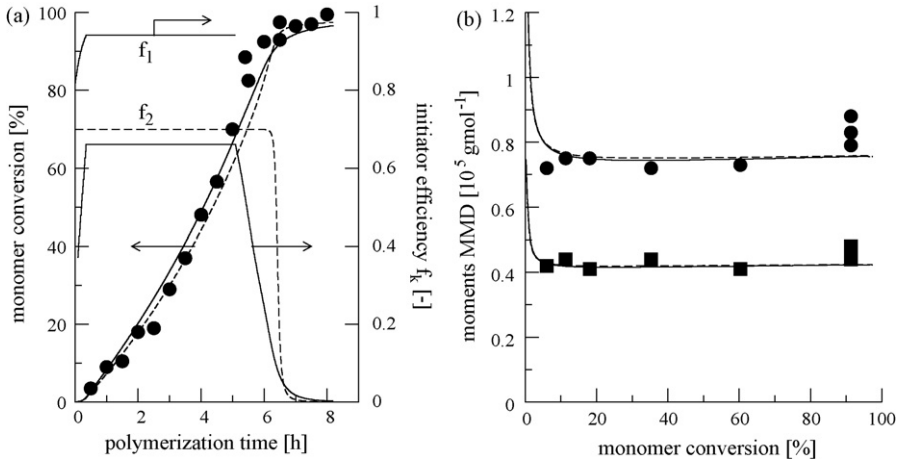

Fig. 7. (a) Monomer conversion and initiator efficiency f_k ($k = 1, 2$) as a function of polymerization time and (b) averages of the MMD as a function of monomer conversion in vinyl chloride suspension polymerization with initiator dodecanoyl peroxide (LPO). Experimental: (a) ●, monomer conversion; (b) ●, M_m; ■, M_n. Calculated: (a) monomer conversion and initiator efficiency f_k; (b) averages of the MMD. Monomer conversion and averages of the MMD calculated by integration of equations in Table S.4 with the set of intrinsic Arrhenius parameter values given in Table S.2; (solid lines) using f_k calculated from Eq. (18) with Arrhenius parameters as shown in Table 1; (dashed lines) using f_k calculated from Eq. (2) with $f_{chem} = 0.7$. Polymerization temperature 333 K, initiator concentration 0.26 wt% based on the monomer. [16].

f_2 based on Eq. (2) starts to decrease at the start of the third stage of the polymerization (i.e. 64% monomer conversion), whereas f_2 from Eq. (2) only starts to decrease from a monomer conversion of 85% on. Also, the decrease of f_2 based on Eq. (18) is less fast as a function of monomer conversion as compared to f_2 based on Eq. (2).

Fig. 8 shows the net rate of radical formation and the radical concentration in the polymer-rich phase using both initiator efficiency models. From this figure it can be seen that the net rate of radical formation using both initiator efficiency models remains identical until the start of the third stage of the polymerization process, i.e. approximately 64% monomer conversion (this corresponds to a polymerization time of 5 h). From this moment on the f_2 value obtained from Eq. (18) starts to decrease, whereas f_2 from Eq. (2) remains constant. Hence, the net rate of radical formation using the f_2 value obtained from Eq. (2) becomes higher as compared to the net rate of radical formation using Eq. (18). At

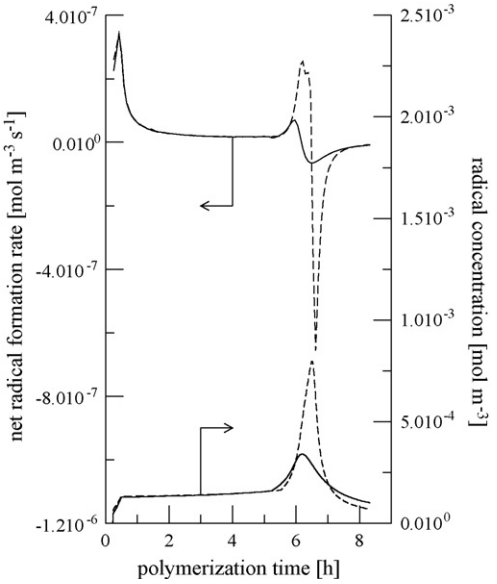

Fig. 8. Net radical formation rate and radical concentration in the polymer-rich phase. Solid lines using initiator efficiency model from Eq. (18); dashed lines using initiator efficiency model from Eq. (2). All lines calculated by integration of equations in Table S.4. Reaction conditions as mentioned in Table 2.

monomer conversions higher than 85% the opposite becomes true. This can be explained by the drastic decrease of f_2 as a function of monomer conversion based on Eq. (2). Due to these differences in the net rate of radical formation in the polymer-rich phase, the radical concentration in the polymer-rich phase varies differently using both models. During the majority of the third stage of the polymerization process the calculated radical concentration in the polymer-rich phase is higher using Eq. (2) to calculate the initiator efficiency. This leads to a different monomer conversion profile, as can be seen from Fig. 7(a). Due to the higher radical concentration in the polymer-rich phase using the intiator efficiency model of De Roo et al. (i.e. Eq. (2)) the polymerization process slows down from a slightly higher monomer conversion onwards. Moreover, due to the drastic decrease of f_2 using the model of De Roo et al., the slowing down of the polymerization process occurs more rapidly.

The different functional form of both initiator efficiency models also results in a different temperature dependence. It can therefore be expected that the calculated initiator efficiencies, and hence monomer conversion profiles, will differ significantly given a larger temperature range as compared to that presented in Section 3.1. Therefore, model calculations for the LPO initiator using both initiator efficiency models have been performed within the industrially relevant temperature range of 310–350 K. From these calculations it could be concluded that significant differences between the calculated monomer conversion profiles using both initiator efficiency models occur, whereas the calculated averages of the MMD remain rather invariant. As can be seen from Fig. 9 the largest differences are observed at the lowest investigated polymerization temperature (310 K). At these low polymerization temperatures the calculated f_2 value from Eq. (18) is significantly lower as compared to that obtained from Eq. (2). Therefore, the increase of the monomer conversion profile is steeper when using Eq. (2). At higher polymerization temperatures the difference between both calculated f_2 values becomes less pronounced, resulting in smaller differences of the calculated monomer conversion profiles.

3.2.2. Benzoyl peroxide initiator (BPO)

Fig. 10 shows for the BPO initiator a comparison of experimental data for the monomer conversion with calculated profiles using both initiator efficiency models. The full lines in this figure represent calculations based on the initiator efficiency model presented in Section 2.2(i.e. Eq. (18)), whereas the dashed lines correspond to the initiator efficiency model in Eq. (2). It can be concluded that

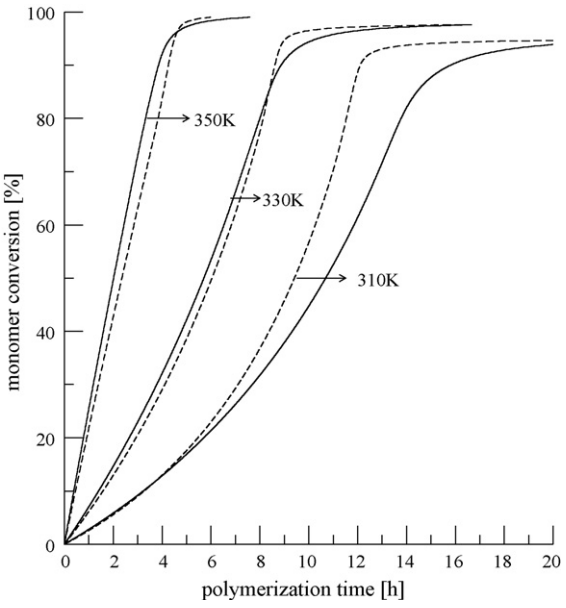

Fig. 9. Monomer conversion as a function of polymerization time in vinyl chloride suspension polymerization with initiator dodecanoyl peroxide (LPO). All lines calculated by integration of equations in Table S.4 with the set of intrinsic Arrhenius parameter values given in Table S.2; (solid lines) using f_k calculated from Eq. (18) with Arrhenius parameters as shown in Table 1; (dashed lines) using f_k calculated from Eq. (2) with $f_{chem} = 0.7$. Polymerization conditions: 310 K, 2.0 wt% LPO; 330 K,0.2 wt% LPO; 350 K, 0.08 wt% LPO.

both initiator efficiency models allow for a good agreement with experimental data.

Fig. 10 also shows the calculated initiator efficiency profiles. The calculated f_1 value resulting from Eq. (18) is slightly lower than 1.

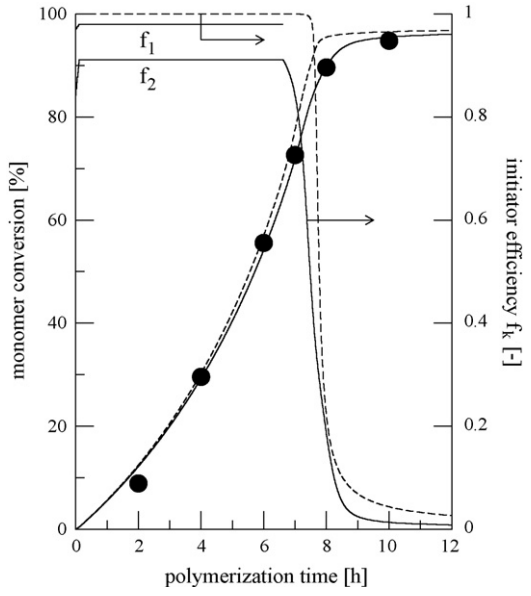

Fig. 10. Monomer conversion and initiator efficiency f_k ($k = 1, 2$) as a function of polymerization time in vinyl chloride suspension polymerization with initiator benzoyl peroxide (BPO). Experimental: ●, monomer conversion. Calculated: monomer conversion and initiator efficiency f_k ($k = 1, 2$), calculated by integration of equations in Table S.4 with the set of intrinsic Arrhenius parameter values given in Table S.2; (solid lines) using initiator efficiency f_k, calculated from Eq. (18) with Arrhenius parameters as shown in Table 1; (dashed lines) using f_k calculated from Eq. (2). Polymerization temperature 323 K, initiator concentration 2.0 wt% based on the monomer.

For the variation of the f_2 value as a function of polymerization time similar conclusions can be drawn as compared to the LPO initiator. The f_2 value resulting from Eq. (18) is lower than that obtained from Eq. (2) and starts to decrease from the start of the third stage on (after approximately 6 h), whereas the latter only decreases from a monomer conversion of ≈ 85% on (this corresponds to a polymerization time of approximately 7 h). However, contrary to the LPO initiator, the efficiency of the BPO initiator according to the model of De Roo et al. (i.e. Eq. (2)) is in both phases higher than the f_k according to the model described in Section 2.2 at all times. Hence, the conversion profile using the former model is higher as compared to that of the latter at all times during the polymerization process. This leads in this case to a better description of the monomer conversion at high monomer conversions when using the initiator efficiency model described in Section 2.2.

4. Conclusions

Calculation of the initiator efficiency is possible based on a kinetic model for the decomposition of the initiator and for the consecutive reactions of the decomposition products. By explicitly accounting for diffusion phenomena the cage effect can be quantified. The latter causes a drastic decrease of the initiatior efficiency and, hence, causes the polymerization process to stop at monomer conversions below 100%.

The proposed methodology and the derived rate equations have been validated for typical industrial initiators but can be extended to any initiator in a straightforward manner.

Acknowledgement

J. Wieme is a Postdoctoral Researcher of the Fund for Scientific Research-Flanders (F.W.O.-Vlaanderen).

Appendix A. Supplementary Data

Supplementary data associated with this article can be found, in the online version, at doi:10.1016/j.cej.2009.06.004.

References

[1] G.T. Russell, D.H. Napper, R.G. Gilbert, Macromolecules 21 (1988) 2133–2140.
[2] T. De Roo, G.J. Heynderickx, G.B. Marin, Macromol. Symp. 206 (1) (2004) 215–228.
[3] C. Reichardt, Solvents and Solvent Effects in Organic Chemistry, Third, updated and enlarged ed., New York, Wiley, 2003.
[4] T. De Roo, J. Wieme, G.J. Heynderickx, G.B. Marin, Polymer 46 (2005) 8340–8354.
[5] J.A. Biesenberger, D.H. Sebastian, Principles of Polymerization Engineering, Wiley, New York, 1983.
[6] N. Tefera, G. Weickert, K.R. Westerterp, J. Appl. Polym. Sci. 63 (12) (1997) 1649–1661.
[7] N. Tefera, G. Weickert, K.R. Westerterp, J. Appl. Polym. Sci. 63 (12) (1997) 1663–1680.
[8] D.S. Achilias, C. Kiparissides, Macromolecules 25 (1992) 3739–3750.
[9] D.L. Kurdikar, N.A. Peppas, Macromolecules 27 (1994) 733–738.
[10] F.C. Collins, G.E. Kimball, J. Colloid Sci. 4 (1949) 425–437.
[11] G. Moad, D.H. Solomon, The Chemistry of Free Radical Polymerization, 1st ed., Pergamon Elsevier Science Ltd., Oxford, UK, 1995.
[12] M. Buback, M. Egorov, V. Kaminsky, O.F. Olaj, G.T. Russell, P. Vana, G. Zifferer, Macromol. Chem. Phys. 203 (2002) 2570–2582.
[13] M. Buback, Macromol. Symp. 226 (2005) 121–132.
[14] M. Buback, M. Kling, S. Schmatz, Z. Phys. Chem. 219 (2005) 1205–1222.
[15] J.K. Kochi (Ed.), Free Radicals, John Wiley & Sons, Inc, New York, 1973.
[16] A.F. Cebollada, M.J. Schmidt, J.N. Farber, N.J. Capiati, E.M. Vallés, J. Appl. Polym. Sci. 37 (1989) 145–166.
[17] A. Crosato-Arnaldi, P. Gasparini, G. Talamini, Macromol. Chem. 117 (2801) (1968) 140–152.
[18] J.S. Vrentas, C.M. Vrentas, Eur. Polym. J. 34 (5/6) (1998) 797–803.
[19] D.W. Van Krevelen, Properties of Polymers—Their Correlation with Chemical Structure; Their Numerical Estimation and Prediction from Additive Group Contributions, Third, completely revised ed., Elsevier, Amsterdam, 1997.